Experimental study of β-delayed proton decay of ^{23}Al for nucleosynthesis in novae

A. Saastamoinen,[1,*] L. Trache,[2] A. Banu,[2,†] M. A. Bentley,[3] T. Davinson,[4] J. C. Hardy,[2] V. E. Iacob,[2] M. McCleskey,[2] B. T. Roeder,[2] E. Simmons,[2] G. Tabacaru,[2,‡] R. E. Tribble,[2] P. J. Woods,[4] and J. Äystö[1]

[1]*Department of Physics, University of Jyväskylä, P.O. Box 35 (YFL), FI-40014 Finland*

[2]*Cyclotron Institute, Texas A&M University, College Station, Texas 77843-3366, USA*

[3]*Department of Physics, University of York, Heslington, York YO10 5DD, United Kingdom*

[4]*School of Physics and Astronomy, University of Edinburgh, Edinburgh EH9 3JZ, United Kingdom*

(Received 21 December 2010; published 27 April 2011)

The β-delayed γ and proton decay of ^{23}Al has been studied with an alternative detector setup at the focal plane of the momentum achromat recoil separator MARS at Texas A&M University. We could detect protons down to an energy of 200 keV and determine the corresponding branching ratios. Contrary to results of previous β-decay studies, no strong proton intensity from the decay of the isobaric analog state (IAS) of the ^{23}Al ground state at $E_x = 7803$ keV in ^{23}Mg was observed. Instead we assign the observed low-energy group $E_{p,\mathrm{c.m.}} = 206$ keV to the decay from a state that is 16 keV below the IAS. We measured both proton and gamma branches from the decay of this state at $E_x = 7787$ keV in ^{23}Mg, which is a very rare case in the literature. Combining our data with its measured lifetime, we determine its resonance strength to be $\omega\gamma = 1.4^{+0.5}_{-0.4}$ meV. The value is in agreement with older direct measurements, but disagrees with a recent direct measurement. This state is the most important resonance for the radiative proton capture ^{22}Na$(p,\gamma)^{23}$Mg in some astrophysical environments, such as novae.

DOI: 10.1103/PhysRevC.83.045808 PACS number(s): 26.50.+x, 23.40.−s, 23.50.+z, 27.30.+t

I. INTRODUCTION

Classical novae are explosive events that appear on interacting binary systems where hydrogen-rich material accretes on a white dwarf from its low-mass main-sequence companion. The accreted hydrogen-rich matter compresses, leading eventually to a thermonuclear runaway [1]. An understanding of the dynamics of nova outbursts and of the nucleosynthesis fueling them is crucial in testing our understanding of the dynamics of stellar phenomena in general. A few classical novae per year are detected in our galaxy, making them a relatively frequent phenomenon, being observed throughout the whole electromagnetic spectrum, and therefore our models can be compared more easily with observations. The composition of the nova ejecta between ^{20}Ne and ^{27}Al depends greatly on the cyclic nuclear-reaction chains beyond the carbon-nitrogen-oxygen (CNO) cycle: namely, the so-called neon-sodium (NeNa) and magnesium-aluminum (MgAl) cycles. The MgAl cycle is crucial for the synthesis of ^{26}Al ($T_{1/2} = 0.7$ My) and the NeNa cycle is relevant for the synthesis of ^{22}Na ($T_{1/2} = 2.6$ y). Both ^{26}Al and ^{22}Na could be detected by space-based γ-ray telescopes through their characteristic γ-rays following β decay. The short half-life of ^{22}Na raises the possibility of detecting it as a pointlike source since it decays before spreading away from the site of its synthesis. The amount of ^{22}Na created in novae may also be relevant for explaining nonstandard ^{22}Ne abundances in the Ne-E meteorites [2].

So far, there are no confirmed observations of γ rays of novae origin [3,4]. However, there is a recent, disputed report about the possible detection of the 1275 keV line from ^{22}Na decay, but it appears to originate from a diffused (not pointlike) source, most likely from the photo-activation of ^{22}Ne by cosmic rays [5]. The NeNa cycle, illustrated in Fig. 1, proceeds along the path of stable nuclei via the reaction chain ^{20}Ne$(p,\gamma)^{21}$Na$(\beta^+\nu)^{21}$Ne$(p,\gamma)^{22}$Na$(\beta^+\nu)^{22}$Ne$(p,\gamma)^{23}$Na$(p,\alpha)^{20}$Ne. When the temperature rises, however, proton capture starts to compete with β decay, and the proton-capture reactions move the reaction products higher in mass, bypassing ^{22}Na. This leads eventually into the MgAl cycle and to a reduced abundance of ^{22}Na in the end products. The rates of these depleting reactions have been of considerable interest, and recent studies include ^{21}Na$(p,\gamma)^{22}$Mg [6,7], ^{22}Mg$(p,\gamma)^{23}$Al [8–10], ^{22}Na$(p,\gamma)^{23}$Mg [11–18], ^{23}Na$(p,\gamma)^{24}$Mg [19], and ^{23}Mg$(p,\gamma)^{24}$Al [20]. It is believed that novae could become the first type of explosive process for which all the nuclear input to the nucleosynthesis calculations is based on experimental data [21].

At typical nova peak temperatures (0.1–0.4 GK), the main destruction channel for ^{22}Na is thought to be the radiative proton capture ^{22}Na$(p,\gamma)^{23}$Mg. This reaction rate is dominated by the capture through narrow and isolated low-energy proton resonances, which correspond to the excited states near the proton-separation threshold in ^{23}Mg. The presently accepted reaction rate for ^{22}Na(p,γ) is based on challenging direct measurements with a radioactive ^{22}Na target [11,14] supplemented by information from indirect measurements, via reaction [12,16,22] and β-decay studies [13,15,17].

The β decay of ^{23}Al populates excited states of ^{23}Mg that can decay by both proton and γ emission. Proton emission following the β decay of ^{23}Al was reported by Gough *et al.* in Ref. [23], where a single proton line at $E_{p,\mathrm{c.m.}} = 870(30)$ keV,

*antti.j.saastamoinen@jyu.fi

†Present address: Department of Physics and Astronomy, James Madison University, Harrisonburg, Virginia 22807, USA.

‡On leave from National Institute of Physics and Nuclear Engineering (IFIN-HH), Bucharest, Romania.

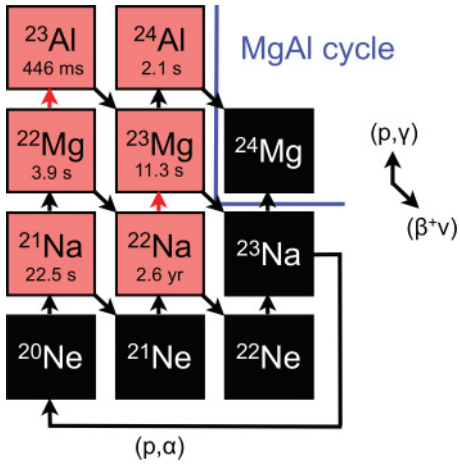

FIG. 1. (Color online) NeNa cycles and possible depleting reactions for stable (black boxes) and β-emitting (red boxes) nuclei.

with $T_{1/2} = 470(30)$ ms, was reported. Since then, three studies have been reported for the β decay of ^{23}Al [13,15,17]. Tighe *et al.* [13] used the helium jet technique with ΔE-ΔE-E Si telescopes, and reported four proton groups with $E_{p,\mathrm{lab}} =$ 223(20), 285(20), 560(5), and 839(5) keV, with a very high intensity for the lowest line, which was assigned to the decay from the isobaric analog state (IAS) of the ground state of ^{23}Al. Peräjärvi *et al.* confirmed these groups and added a few more by using a ΔE-E gas-Si telescope with the Ion Guide Isotope Separator On-Line (IGISOL) technique [15], giving a total of six proton groups at $E_{p,\mathrm{lab}} = 200(20)$, 270(20), 400(20), 554(7), 839(6), and 1931(14) keV. In addition, five γ rays, including one attributed to the decay of the IAS, were reported. However, contrary to the previous study, they did not observe a high intensity for the lowest-energy proton group, which was also assigned to the decay of the IAS. The most recent study was by Iacob *et al.* [17], in which β-delayed γ rays were measured in close geometry from a high-purity source produced with a recoil separator. The ground-state spin and parity of ^{23}Al were determined to be $5/2^+$, in agreement with a β-NMR study [24], and the half-life was improved to $T_{1/2} = 446(6)$ ms. This study also identified both the 7787(2)-keV and the 7803(2)-keV (IAS) states at the same time, though both had been observed separately in previous studies [14–16].

In this paper, we report an alternative measurement to address the discrepancies in proton intensities around 200 keV above the proton-separation threshold in ^{23}Mg, and to determine absolute proton-decay branchings by combining our data with the results from an extended analysis [25] of the decay data published originally in [17]. Implications of our results on the ^{22}Na(p,γ) reaction rate are discussed.

II. EXPERIMENTAL TECHNIQUE

The experiment was conducted at the Cyclotron Institute of Texas A&M University. The K500 superconducting cyclotron and the momentum achromat recoil separator (MARS) [26] were used to produce the nuclei of interest and implant them in our detector setup. The ^{23}Al secondary beam was produced the same way as it was in our earlier experiments described in Ref. [17] (and references therein). We used the ^{1}H(^{24}Mg,^{23}Al)2n reaction in inverse kinematics by bombarding a 2.5 mg/cm^2-thick, liquid-nitrogen-cooled H_2 target at 1.6 atm pressure with a ^{24}Mg beam at 48 MeV/u. The resulting reaction products were guided through a dipole-quadrupole-dipole momentum achromat, a Wien filter, and a final dipole, to yield a beam of up to 4000 ^{23}Al ions/s at 42 MeV/u with purity of better than 90% and a momentum spread $\Delta p/p = \pm 0.6\%$. See Fig. 2.

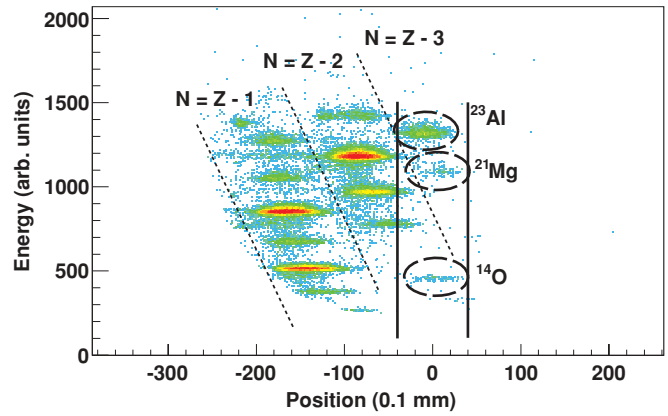

FIG. 2. (Color online) Secondary-beam identification with the ΔE-E target telescope at the focal plane of MARS. The vertical bars represent the position of the momentum-defining slits in MARS during the production of ^{23}Al. This setting yields $\Delta p/p = \pm 0.6\%$ and a purity of better than 90%.

The implantation chamber, which was installed into the focal plane of MARS, housed a rotatable degrader system and our detector setup. A schematic presentation of the setup is given in Fig. 3. The radioactive species in the beam were

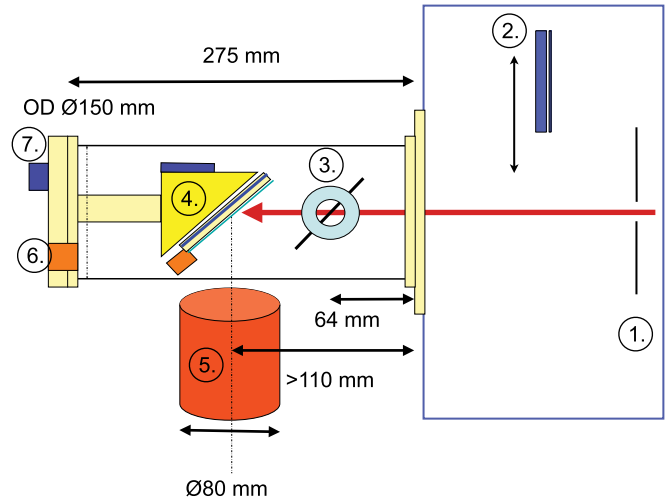

FIG. 3. (Color online) Schematic representation of the detector setup at the focal plane of MARS: (1) Separator *XY* slits, (2) ΔE-E detector for beam tuning, (3) Rotatable aluminum degrader, (4) 45° wedge with the detector stack, (5) HPGe detector, (6) Cabling connections, and (7) Cooling system. See text for more details.

first identified with reduced beam intensity in a ΔE-E target telescope placed in front of the detector setup. After the separator had been adjusted so that only the wanted activity went through the last pair of slits, the telescope was moved away and the beam was allowed to pass into the implantation chamber. The beam then traveled through an 820-μm Al degrader, which we used to control the implantation depth into the detector stack. The angular resolution of the rotating degrader system is 0.1°.

The detector stack consisted of a double-sided silicon strip detector (DSSSD) and a thick silicon pad detector. The DSSSD we used was a 69-μm-thick Micron W1 with $16(x) + 16(y)$ 3.1×50 mm^2 strips, and the Si pad was 998-μm thick, with a surface area of 50×50 mm^2. The detector stack had cooling capability and was mounted on a platform at a 45° angle in order to increase the effective implantation thickness and allow for a good gamma-ray efficiency for a 70%-relative-efficiency, high-purity germanium (HPGe) detector installed outside the chamber as close as physically possible (11 cm).

The two Si detectors were used in two different modes: an "implantation control mode" and a "measurement mode." In the first mode, we used them as a ΔE-E telescope to control the implantation of the beam of interest midway into the DSSSD by adjusting the implantation depth with the rotating Al degrader and observing the beam spot to move first in the two-dimensional, energy-loss-vs-energy plot relating the signals from both detectors, and later in the DSSSD alone. As a result of these measurements, we decided to reduce the momentum spread of the beam from $\Delta p/p = \pm 0.6\%$ to $\pm 0.25\%$ by closing the momentum-defining slits after dipole 1 of MARS. This both reduced the rate of ^{23}Al nuclei striking the detector at 42 MeV/u down to 600–800 pps and narrowed the depth distribution of the implanted ^{23}Al to ∼17 μm, full width at half maximum (FWHM) (in agreement with the results of our simulations). Under these conditions, we calculated that protons emitted with energies $E_p < 1.4$ MeV would be fully stopped in the DSSSD. In the measurement mode, the thick Si pad served as a β detector in our actual measurements.

During the experiment, the beam was pulsed: the desired activity was implanted into the detector for one second, followed by a 5-ms wait. Decays from the sample were then recorded for one second, yielding a duty cycle of 50%. All the data were collected with a condition of logical OR between β-p coincidences and β-γ coincidences. The secondary-beam intensity was limited to a few hundred ions per second, and the implantation spot was spread over several strips to reduce damage to the DSSSD. This helped also to keep the acquisition count rate at around a few hundred Hz, which resulted in a negligible dead time.

III. RESULTS AND ANALYSIS

A. Gamma-ray spectrum

We calibrated the energy and efficiency of the HPGe detector with standard sources of ^{60}Co, ^{137}Cs, and ^{152}Eu, and checked it during the measurement with the known γ-ray lines from ^{24}Al. The resultant efficiency calibration had an uncertainty of 1% in the 450-keV region and, since the γ-ray spectrum is very well known from previous experiments [17,25], this was sufficient for us to calibrate our full spectrum. The β-gated γ-ray spectrum from ^{23}Al decay in this experiment is presented in Fig. 4. In this spectrum we can identify the strongest transitions at 451, 1600, and 2050 keV, as well as the 5751, 7351, and 7801-keV transitions originating from the IAS, and the 5736 and 7335-keV transitions from the 7787-keV state just below the IAS (see Fig. 5). Our measured intensities for the γ-ray lines at 1600 and 2050 keV, relative to the line at 451 keV, agree with the previous studies [15,17,25].

The only impurity present in larger quantities in the stopped beam, ^{14}O, is identified in the γ-ray spectrum through the 2313-keV line, which follows its β decay. There is also a tiny amount of ^{22}Mg stopped into the thick Si detector, because few tens of 583-keV γ rays from ^{22}Na are observed without any proton coincidences. The γ rays that follow the β decay of ^{23}Mg, most notably the one at 439 keV, are also present since this daughter activity stays in the detector. We do not observe the 2317, 5055, 5067, and 5729-keV γ-ray transitions observed in Ref. [16]. This is not surprising since these γ-ray transitions originate from the states at 7769.2(10) and 7779.9(9) keV, whose spin assignments are $9/2^+$ and $11/2^+$ respectively: Their population in β decay would be negligible.

B. Proton spectrum

Energy calibration for the DSSSD was done with known β-delayed protons from the decay of ^{21}Mg [27], which have energies of 1257(10), 1773(2), and 1939(5) keV (see Fig. 6). The 554(6) and 839(7)-keV proton lines from the decay of ^{23}Al [15] were also used as an internal calibration to obtain a more reliable extrapolation down to the interesting energy region around 200 keV. The ^{21}Mg beam, which is only a weak byproduct of our reaction (see Fig. 2), has a range in Al of about 100 μm longer than ^{23}Al. By adjusting the energy degrader, we could tune it into the middle of the DSSSD, albeit with a meager rate of ∼1 pps. The spectrum we obtained in one 8-hour measurement appears in Fig. 6. These lines altogether yield a calibration that has an uncertainty of about 8 keV down to the 200-keV region. The thick Si pad was calibrated with known α energies from the β-delayed α decay of ^{20}Na.

When a decay with proton emission happens in the middle of the detector, the observed total decay energy is a sum of the proton, the recoiling daughter nucleus, and the energy $E_{\langle\beta\rangle}$ that the preceding β particle deposits in the detector. If we assume that the decay takes place at rest and that the recoil from β decay is negligible, then after proton emission, the recoiling daughter nucleus has an energy equal to $(M_p/M_{\rm rec})E_p$, where M_p and E_p are the proton mass and energy and $M_{\rm rec}$ is the recoil nucleus mass. However, some of the kinetic energy of the daughter nucleus is not recorded by the detector because the heavy ion loses a fraction of its energy to the silicon lattice rather than to charge-carrier formation (ionization). We obtained this fraction k from a TRIM [28] computation for the relevant recoil energies. Thus we can write the energy we measure in the detector as

$$\begin{aligned} E_{\rm meas} &= E_p + kE_{\rm recoil} + E_{\langle\beta\rangle} \\ &= \left(1 + k\frac{M_p}{M_{\rm rec}}\right) E_p + E_{\langle\beta\rangle}. \end{aligned} \quad (1)$$

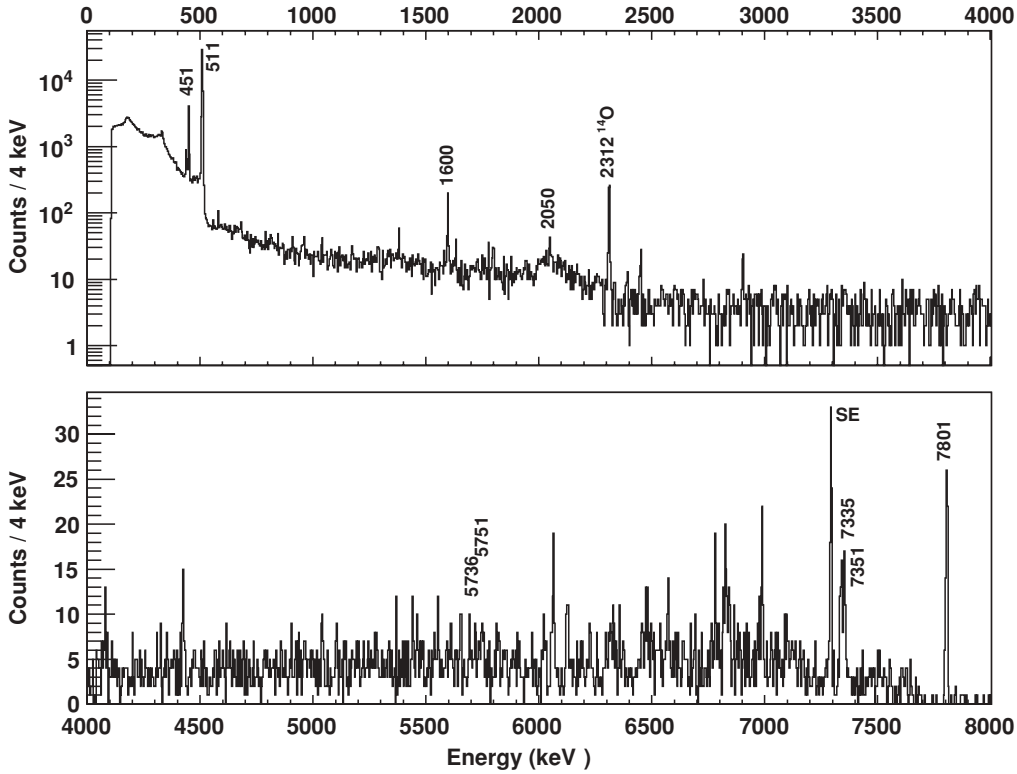

FIG. 4. The γ-ray spectrum following the β decay of ^{23}Al from 0–4 MeV (upper panel, log scale) and 4–8 MeV (lower panel, linear scale). Major γ lines relevant for the states near S_p are identified, as well as the only major contaminant present, ^{14}O ($E_\gamma = 2313$ keV). See text for more details.

As the Q values of the decaying systems are of the order of several MeV and up, the majority of the β particles are minimally ionizing particles and leave on average 13 keV in a half thickness of the DSSSD. Their spectrum is a continuum, which produces a tail on the right-hand side of each proton peak.

We could clean the proton spectrum considerably by requiring that the multiplicity of each recorded event in the DSSSD be one, and that the energies of the front and back sides of the DSSSD be consistent with each other (i.e., $E_x = E_y$). This means that instead of looking at only 16 separate

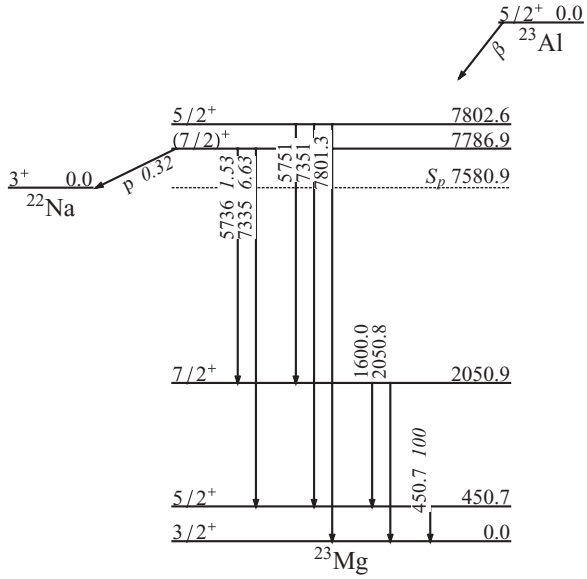

FIG. 5. Partial level scheme of ^{23}Mg. The transition intensities (in italics, percents relative to the 451-keV line) for the astrophysically relevant 7787-keV state are shown; γ intensities and energies are from Ref. [25] and the proton intensity from this work.

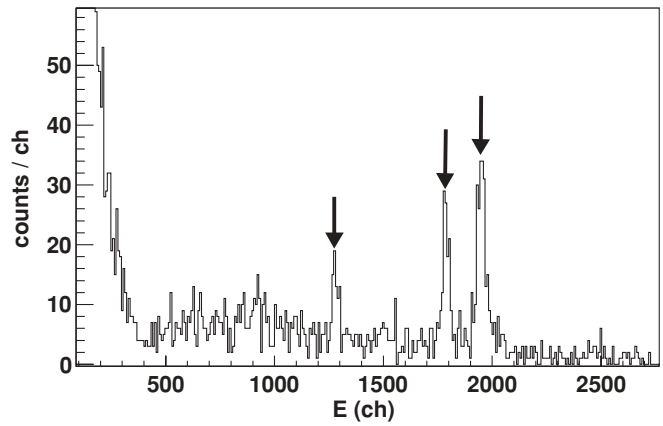

FIG. 6. A sample β-delayed proton spectrum obtained from the decay of ^{21}Mg. The ^{21}Mg ions were deposited midway through the DSSSD and the decay spectrum was acquired with one strip over about 8 hours of beam time. The known 1257(10), 1773(2), and 1939(5)-keV lines [27] are highlighted with arrows.

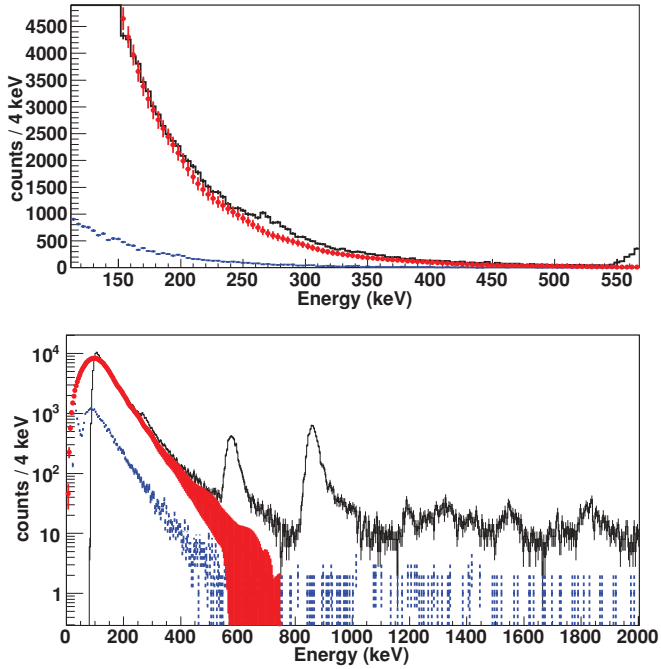

FIG. 7. (Color online) Full collected statistics for the ^{23}Al data (black solid line) and the ^{22}Mg data (blue dashed line). The energy is the total measured decay energy. The smoothed ^{22}Mg spectrum, scaled to match the ^{23}Al spectrum at 150 keV, is shown with red dots and corresponding uncertainties. The upper panel shows only the low-energy part where the proton group at ~270 keV is clearly visible on top of the β background, whereas the lower panel shows the total spectra.

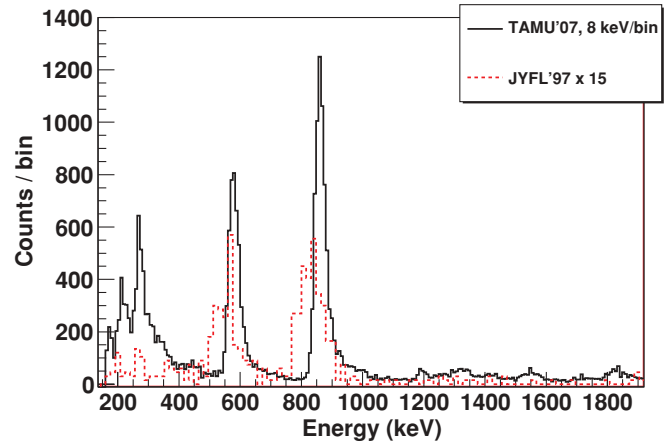

FIG. 8. (Color online) Comparison of the β-delayed proton spectrum of ^{23}Al obtained in this experiment (black solid line) and the spectrum published in [15], which has been magnified 15 times (red dash line). The peaks from this work are slightly higher in energy because they represent the total measured decay energy, whereas in [15], the spectrum was obtained from a detector outside the source, which recorded only the proton energy. The original data for this plot is courtesy of Peräjärvi [30].

strips, we look into 256 separate pixels, each of size ~3.1 × 3.1 mm^2. Still, the pixel volume of the DSSSD used was fairly large and, as can be seen in the top panel of Fig. 7, its β response yields a considerable background extending all the way up to about 400 keV in the ^{23}Al proton spectrum. To look for the astrophysically interesting proton energies, we had to use background subtraction. In this case, we measured the β response of the detector by using ^{22}Mg, which β decays to excited states of ^{22}Na emitting only γ rays. Simulations have shown that the energy-loss spectra of the emitted positrons are very similar in the two cases, and the measurements confirmed that. The measured β spectrum from ^{22}Mg had to be smoothed to get rid of the statistical fluctuations, and then it had to be scaled to match the background from the decay of ^{23}Al. The background shape estimation, smoothing, and scaling were done with standard tools found in the ROOT data-analysis framework [29] and the result is shown in the bottom panel of Fig. 7, where the total counts obtained for both ^{23}Al and ^{22}Mg in the low-energy region are plotted together with the smoothed ^{22}Mg spectrum before and after the scaling operation.

The original data has a statistical error of $\sqrt{N}$ for each bin and the errors are propagated through the smoothing and subtraction routine for each bin individually. The uncertainties after the background subtraction are about three times larger than the bare statistical error. This yields a more realistic estimate for the uncertainties in the fitted peaks. The backgrounds were chosen to be matched around 150 keV, which is above our worst noise conditions (and thus our trigger thresholds) and low enough not to be in the region of the interesting proton lines.

The intensities of the two strongest known proton lines were used to check that no relevant data had been lost as the different conditions were applied to the data, and the background subtracted. No significant changes were observed. Our simulations show that below $E_p = 1.0$ MeV, we miss less than 4%, and for $1.0 < E_p < 1.5$, we lose 5–10%, and have corrected for it. The losses are due to the incomplete charge collection of the events taking place in the interface of the adjacent strips and for protons that leave the detector. The uncertainty of these corrections does not add considerably to the overall uncertainties. The resulting background-reduced spectrum for the β decay of ^{23}Al is presented in Fig. 8 and compared with the one from Ref. [15]. The data from the present work is clearly closer to the spectrum presented in Ref. [15] than to the spectrum in Ref. [13], in which significant noise at low energy was evidently interpreted as a peak at $E_{p,\mathrm{lab}} = 223$ keV.

In our measurement, β particles were always present and summed up with the measured protons, resulting in proton peaks that do not follow a pure Gaussian shape. Instead the peaks have a tail on the high-energy side, which can be described with a skewed Gaussian peak shape,

$$f(E) = \frac{1}{\sqrt{2\pi}\sigma}\exp\left[-\frac{1}{2}\left(\frac{E-\mu}{\sigma}\right)^2\right] \quad \text{for} \quad E \leqslant \mu + a\sigma,$$
$$f(E) \propto |E-\mu|^{-n} \quad \text{for} \quad E > \mu + a\sigma, \qquad (2)$$

where E is energy and all other symbols are parameters for the peak shape and location. The background-subtracted spectrum

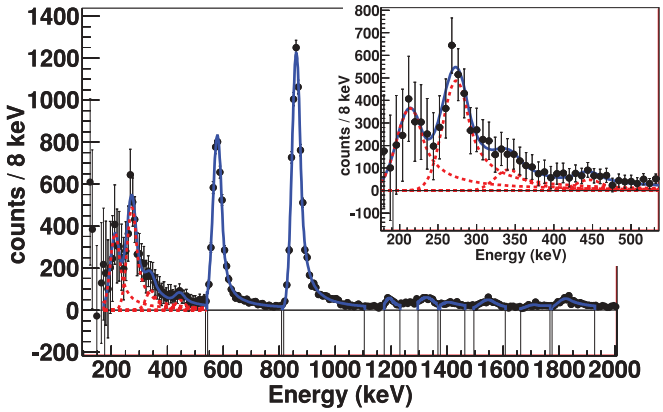

FIG. 9. (Color online) Spectrum for β-delayed protons from ^{23}Al obtained after background subtraction. The energy shown is the total measured decay energy. The fits appear as solid lines. The inset shows the composite fit consisting of presumed peaks in the low-energy part where significant background subtraction was required.

with fits to the identified proton lines is shown in Fig. 9. The major peaks around 580 and 860 keV were fitted first to obtain information about the peak-shape parameters. Then, assuming that the peak shape is independent of decay energy, we used the same parameter values for the other peaks.

The peak around 270 keV can be used as an additional check for our background subtraction. This peak is visible as a clear "bump" on top of the β continuum in the raw data presented in Fig. 7, and it can be fitted with a shape described by Eq. (2) on top of a simple background of an exponential shape. The values for the peak centroid and area obtained by this procedure were in excellent agreement with the results obtained from the background-subtracted fit previously described. Based on this test and the others already mentioned, we conclude that the intensities of the proton peaks around 200 keV obtained from the background-subtracted spectrum have an uncertainty of 20% or better. The results obtained from our fits are presented in Table I, where we give the observed peak centroids, deduced center-of-mass proton energies, energies of the intermediate excited states in ^{23}Mg, proton intensities relative to the 451-keV γ transition, and absolute intensities from each state. The uncertainties quoted for the decay energies are quadratic sums of the uncertainties from the calibration and the fit. Uncertainties from the calibration dominate in the region where no background reduction was made, whereas in the background-subtracted region, the fitting error impacts the uncertainty. As the masses of the proton and of ^{22}Na are known to high precision [31,32], their contributions to the uncertainties in the emitted-proton energies are negligible (though still included in the calculations). The energies of the excited states in ^{23}Mg are $E_{\rm ex}(^{23}{\rm Mg}) = E_{p,{\rm c.m.}} + S_p(^{23}{\rm Mg})$, where $S_p(^{23}{\rm Mg}) = 7580.9(7)$ keV [31–33]. We calculated the relative intensities of the proton groups by normalizing the fitted peak areas to the observed number of 451-keV γ rays. We then obtained the absolute branchings from the relative intensities by using $I_\gamma(451) = 43.3(10)\%$ from Ref. [25], which is a more refined analysis of work originally reported in Ref. [17].

IV. DISCUSSION

A. Comparison with earlier data

It was shown in Ref. [17] that a doublet of states at 7787 and 7803 keV exists (see Fig. 5), of which the second was demonstrated to be the IAS of the $T = 3/2$ ^{23}Al ground state. The energy we obtain for the lowest-measured proton group indicates that these protons originate from a level with an energy of 7787(11) keV instead of the IAS ($E_{\rm ex} =$ 7802.64(48) keV [25,34]), the state to which it was assigned

TABLE I. Measured proton energies and intensities from the β decay of ^{23}Al. $E_{\rm ex}(^{23}{\rm Mg})$ from the present work are calculated with $S_p(^{23}{\rm Mg}) = 7580.9(7)$ keV [31–33]. The relative intensities are normalized to the observed number of 451-keV γ rays, and the absolute branching is based on $I_{\gamma,{\rm abs}}(451) = 43.3(10)\%$ from [25]. See text for more details.

$E_{\rm meas}$ (keV)	$E_{p,{\rm c.m.}}$ (keV)	$E_{\rm ex}(^{23}{\rm Mg})$ (keV)		Relative intensity	Absolute branching (%)
		Present	Adopted[a]		
214(11)	206(11)	7787(11)	7786.86(53)[b]	0.32(6)	0.14(3)
273(9)	267(9)	7848(9)	7854.8(12)	0.42(8)	0.18(4)
341(15)	337(15)	7917(15)		0.08(2)	0.03(1)
446(15)	443(15)	8024(15)	8017.2(12)	0.04(2)	0.02(1)
579(8)	579(8)	8160(8)	8163.3(12)	0.65(2)	0.28(1)
861(8)	866(8)	8447(8)	8453(5)	0.95(3)	0.41(1)
1194(8)	1204(8)	8785(8)	8793(8)	0.04(1)	0.02(1)
1326(9)	1338(9)	8919(9)	8916(6)	0.06(1)	0.02(1)
1405(10)	1419(10)	8999(10)	8990(6)	0.04(1)	0.02(1)
1546(9)	1561(9)	9142(9)	9138(6)	0.06(1)	0.03(1)
1712(25)	1729(25)	9310(25)	9328(8)	0.04(1)	0.02(1)
1824(9)	1843(9)	9424(9)	9420(8)	0.11(1)	0.05(1)
					$\Sigma = 1.22(5)$ %

[a]Latest evaluation of $A = 23$ (Ref. [34]).
[b]Weighted average of data from Refs. [25,34].

TABLE II. Proton energies and intensities obtained in this work compared to the results from previous β-decay studies. All energies are quoted as in the center-of-mass system. Here the intensities from the present work and from Ref. [15] are quoted relative to the 866-keV line to conform with the convention in Ref. [13].

$E_{p,\text{c.m.}}$ (keV)			Relative intensity		
Ref. [13][a]	Ref. [15][a]	Present	Ref. [13]	Ref. [15][b]	Present[c]
233(20)	209(20)	206(11)	2.2(5)	0.10(8)	0.34(6)
298(20)	282(20)	267(9)	0.9(3)	0.13(9)	0.45(9)
		337(15)			0.08(3)
	418(20)	443(15)		0.13(9)	0.04(2)
585(5)	579(7)	579(8)	0.7(1)	0.73(49)	0.69(3)
877(5)	877(6)	866(8)	1.0	1.0	1.0
		1204(8)			0.04(1)
		1338(9)			0.06(1)
		1419(10)			0.05(1)
		1561(9)			0.06(1)
		1729(25)			0.04(1)
		1843(9)			0.11(1)
	1939(14)			0.06(5)	

[a]Originally reported as laboratory energies.
[b]Originally reported as intensities relative to 451-keV γ line.
[c]Calculated from intensities presented in Table I.

in the previous works [13,15]. This identification is based on the energy matching, the fact of the existence of these two states that are 16 keV apart, and the strong population of the lower state in β decay [17,25]. We believe this identification to be better than the 85% confidence given by a standard statistical analysis. A comparison of our proton energies to those given in [13,15] appears in Table II. Both earlier works assigned the protons as being from the IAS, and used arguments based mostly on shell-model calculations with isospin-nonconserving interactions to achieve large-enough isospin mixing to allow isospin-forbidden proton emission in competition with γ-ray emission. With our improved resolution and statistics, we do not see any substantial number of protons originating from the IAS and therefore we cannot support the extraordinarily large isospin mixing claimed in Ref. [13]. Even in the extreme scenario in which the lowest proton peak we see is from the decay of the IAS entirely, the proton branching of that state would be 6–7 times smaller than that published in Ref. [13]. When we add an extra peak to the sum fit shown in Fig. 9 at the energy corresponding to protons possibly originating from the IAS ($E_{p,\text{c.m.}} = 230$ keV), we obtain a relative proton intensity that is consistent with zero ($0^{+0.06}_{-0}$ per one-hundred 451-keV γ rays). While with our typical resolution of 30 keV (FWHM) in the DSSSD used we cannot completely rule out some small contribution from the IAS, we do not find a reasonable argument to believe that of the two states in the doublet in question, the lower state ($T = 1/2$ isospin) does not proton decay, while the (mostly) $T = 3/2$ IAS would, given that the decay of the latter is isospin forbidden. This is an additional argument for our identification.

It can be seen from Table II that our measured relative intensity for the two strongest proton lines agrees with the results presented in Refs. [13,15], but the relative intensities disagree in all other cases, especially with the lowest-energy line as reported in Ref. [13]. Our proton intensities relative to the 451-keV γ transition are somewhat larger than the ones presented in Ref. [15]. This discrepancy can be at least partly due to the conservative ΔE-E gate used to produce the Department of Physics, University of Jyväskylä (JYFL) spectrum [30] and to poor statistics.

We observe all previously identified β-delayed proton groups with emitted proton energy higher than 200 keV, apart from the 1931(14) keV group, which was identified in Ref. [15]. In addition, we find a small peak with $E_{p,\text{c.m.}} = 337(15)$ keV in the tail of the larger 267(9)-keV peak. A higher statistics measurement with the same or better resolution should be made to clarify its existence. In previous reaction studies, the excitation-energy region of this peak has either been covered by a contamination peak (in ^{25}Mg(p,t) [35]) or been unobserved (in ^{24}Mg(p,d) [22]). We also identify six proton groups ($E_p > 1200$ keV) from levels that have only been observed so far in a ^{25}Mg(p,t) measurement [35].

As discussed in Sec. III A, we do not observe any peaks in our γ-ray spectrum that correspond to a transition from the 7769.2(10)-keV $J^\pi = (9/2^+)$ state. There is no evidence either in our proton spectrum of a peak at 198 keV (laboratory energy), which could arise from the decay of that state. In our data, we could in principle detect, with present statistics, at least a contribution from such a proton peak if it were fed strongly. However, we do not see it. This is consistent with the $(9/2^+)$ assignment of Ref. [16] since the state then could not be fed by β decay in our experiment. However, this spin assignment also excludes this state from contributing to the astrophysical reaction rate for radiative proton capture.

B. Resonance strength of the 7787-keV state

We will discuss in more detail the state at $E^* = 7787$ keV because it makes the largest contribution to the astrophysical reaction rate and because, to our knowledge, this is only the second case in the literature in which both proton and γ-ray branches have been measured from the same state simultaneously; the other case known is a state in ^{32}Cl [36]. These situations are rare because of the exponential dependence of the barrier-penetration probability on the proton energy: for larger E_p, most states decay by proton emission, while at lower energies, proton emission is so much hindered that γ-ray emission predominates. Both decay modes are observable only in a very narrow energy window, and it seems that the 7787-keV state in ^{23}Mg with $E_{p,\mathrm{c.m.}} = 206$ keV is within that window.

Typical temperatures in ONe novae are in the region of 0.1–0.4 GK and therefore states up to about 0.9 MeV above the proton-separation threshold in ^{23}Mg may contribute to the radiative proton capture in ^{22}Na$(p,\gamma)^{23}$Mg. However, in practice, the dominant resonances are in the lower end of the Gamow window, where the total width is dominated by the γ-ray partial width. Here the meaningful region is in the neighborhood of the IAS in ^{23}Mg.

The reaction rate for narrow isolated resonances is expressed as

$$N_a\langle\sigma v\rangle = 1.5399 \times 10^{11}(\mu T_9)^{-3/2} \times \sum_i (\omega\gamma)_i \exp(-11.605 E_i/T_9), \qquad (3)$$

where the units are cm^{3}mol^{-1}s^{-1}, μ is the reduced mass of the colliding nuclei in u, T_9 is the temperature in GK, E_i is the center-of-mass energy of the ith resonance, and $\omega\gamma_i$ is the resonance strength of the ith resonance, both in MeV. The resonance strength is defined as

$$\omega\gamma = \frac{2J+1}{(2J_p+1)(2J_t+1)}\frac{\Gamma_p\Gamma_\gamma}{\Gamma_p+\Gamma_\gamma}, \qquad (4)$$

where Γ_p and Γ_γ are proton and γ widths, respectively, of the state. As stated earlier, for the low-resonance energies, the γ width dominates and thus the resonance strength depends only on the proton width, i.e., $\omega\gamma \approx \omega\Gamma_p$, when $\Gamma_p \ll \Gamma_\gamma$.

Since the 7787-keV state is fed in allowed β decay, the positive-parity assignment is solid, as shown in Ref. [17]. Given the selectivity of β decay, the possible spins for this state are 3/2, 5/2, or 7/2. A spin of 3/2 is excluded by the observation of the proton emission to the $J^\pi = 3^+$ ground state of ^{22}Na, since that would require the proton to carry away an angular momentum of $L = 2$. The $5/2^+, T = 3/2$ IAS is only 16 keV higher than the 7787-keV state, and another state with the same spin and parity would cause strong mixing between these states. However, it has been demonstrated that the $A = 23, T = 3/2$ isobaric multiplet, in which the state at 7803 keV is the $T_z = -1/2$ member, obeys the isobaric multiplet mass equation (IMME) to a high precision [33]. Therefore we rule out a spin of 5/2 for the 7787-keV neighboring state and assign it spin parity $(7/2)^+$. This is more restrictive than the currently accepted spin parity for the 7787-keV state $(7/2^+)$ [34]. Based on the proton intensity we observed for the decay of this state and the γ-ray intensities determined in Ref. [25], we obtain a proton branch for this state of 3.7%, and γ branchings of 78.2% and 18.1% to the 451-keV and 2050-keV states, respectively. The relevant part of the decay scheme is shown in Fig. 5 .

The lifetime of the 7787-keV state has been measured to be $\tau = 10(3)$ fs from in-beam γ spectroscopy [16]. Using that lifetime and our measured proton and γ branchings, we derive $\Gamma_\gamma = 63(20)$, $\Gamma_p = 2.5(11)$, and a resonance strength $\omega\gamma = 1.4^{+0.5}_{-0.4}$ meV. This resonance strength for the 7787-keV state agrees with the old value of 1.8(7) meV from the direct measurement reported by Stegmüller *et al.* [14]. However, it differs substantially from the more recent direct measurement by Sallaska *et al.* [18], who measured $\omega\gamma = 5.7^{+1.6}_{-0.9}$ meV for the 7787-keV state, which was 3.2 times the older result. The difference between the latest direct measurement and the earlier one are discussed in detail in Ref. [37]; we discuss here only the possible sources of difference when compared to our work.

The resonance strength we obtained is based on indirect information and combines data from several different experiments. What are the uncertainties related to each source? The lifetime of the 7787-keV state was determined by Jenkins *et al.* [16], who used the Doppler-shift attenuation method (DSAM) [38] under the assumption that feeding to this high-lying unbound state is direct. DSAM is most sensitive in the range from a few fs to a few tens of fs, which coincides with the observed lifetime for the state. However, the uncertainty quoted for this lifetime was 3 fs and represents the major contribution to the uncertainty for the $\omega\gamma$ result derived in this work.

The γ-ray intensities for the 7787-keV state determined in [17,25] were obtained with the same instruments and techniques used for other high-precision β-decay branching-ratio measurements (see, e.g., [39] and references therein). The resultant γ-ray branching ratios disagree only slightly with those reported by Sallaska *et al.* [37]; but they differ considerably from those determined by Jenkins *et al.* [16], who attribute some of the γ lines to a nearby state, which has not been found in any direct measurement, nor was it observed in any β-decay experiments.

The relative proton intensities determined in this work may suffer from the fact that a significant background had to be subtracted in order to analyze the low-energy peaks. Nevertheless, as discussed in Sec. III B, the area determined for the $E_{p,\mathrm{c.m.}} = 267$ keV peak is not altered if a different method is used in its evaluation. It is also worth noting that our uncertainties for the low-energy proton peak intensities are at best just under 20%, yet their contribution to the total error of the resonance strength is small compared with the contribution from the uncertainty in the lifetime. Furthermore, our proton intensity relative to the 451-keV γ-ray line is already somewhat higher than Peräjärvi *et al.* [15], and it is unlikely that we have lost any significant amount of the proton intensity in the lowest-energy proton groups. Therefore, if the resonance strength of the 7787-keV state is indeed as high as claimed in Ref. [18], then the lifetime of the 7787-keV state should be less than its present value.

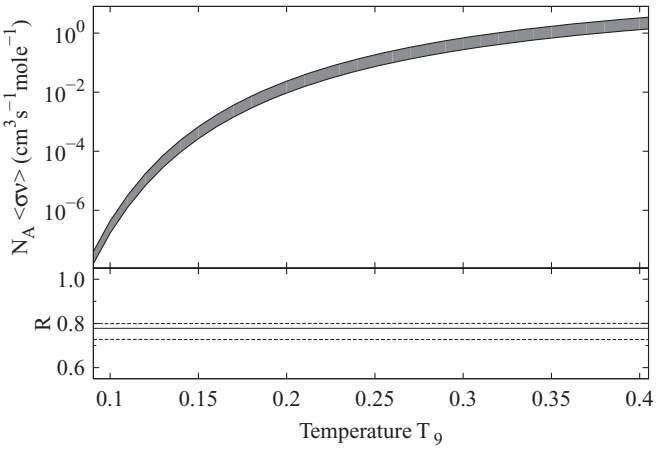

FIG. 10. Upper panel: The contribution of the 7787-keV state to the ^{22}Na(p, γ) reaction rate at typical nova peak temperatures. Lower panel: Ratio ($R = N_a\langle\sigma v\rangle / N_a\langle\sigma v\rangle_{\text{adopted}}$) of the rate deduced in the present work (see text) and the adopted rate [40].

All in all, given the discrepancy between the latest direct measurement of $\omega\gamma$, and both our result and that of Stegmüller *et al.* [14], more indirect data is clearly needed to settle this issue. A new, more precise, level lifetime measurement for the 7787-keV state is called for. Moreover, a measurement of the lifetime of the 7855-keV state would also be beneficial, since its proton intensity is less sensitive to the background present in our measurement.

As our resonance strength agrees with the value adopted in the European Nuclear Astrophysics Compilation of Reaction Rates (NACRE) compilation [40], it does not make a significant change in the reaction rates presented in the compilation, but rather confirms them and reduces their uncertainties (see Fig. 10).

V. CONCLUSIONS

We have used an alternative detector setup to study excited states in ^{23}Mg populated in the β decay of ^{23}Al, and determined the absolute proton-emission branching ratios for several excited states in ^{23}Mg. No anomalously high-intensity proton line from the decay of IAS of ^{23}Al was observed, in contradiction to previous studies [13,15]. Instead we have attributed the previously observed lowest-energy proton group to the decay of the 7787-keV state, which lies 16 keV below the IAS. Our observed intensities for low-energy proton groups are lower than those appearing in Ref. [13], but higher than those in Ref. [15]. The total proton-decay intensity of 1.15(6)% agrees with an earlier estimate from β-delayed γ decay [25], but is higher than the value 0.46(23)% adopted in the Nuclear Data Sheets [34].

Our data is consistent with the earlier high-spin assignment of the state at 7769 keV, and therefore we confirm that it does not contribute to the astrophysical reaction rate of the radiative proton-capture reaction ^{22}Na(p, γ)^{23}Mg. We have measured both the proton and γ-ray branches from the de-excitation of the $J^\pi = (7/2)^+$ state at $E_x = 7787$ keV, which is the resonance with the largest contribution to the reaction rate of the radiative proton-capture reaction ^{22}Na(p, γ)^{23}Mg in hot, astrophysical environments. The extracted resonance strength of this astrophysically interesting state, $\omega\gamma = 1.4^{+0.5}_{-0.4}$ meV, agrees with an old direct measurement [14], but disagrees with the latest one [18]. Solving this discrepancy may require further measurements for the lifetimes of excited states in ^{23}Mg and its mirror nucleus ^{23}Na. A new measurement of the β-delayed protons from ^{23}Al with a detector less sensitive to β particles would help to clarify the existence and strength of the states that are fed weakly. Also, improved resolution is needed to distinguish any possible contribution from protons originating from the IAS in ^{23}Mg. Promising technologies, such as active target systems or superconducting microcalorimeters [41], may make such improvements possible.

ACKNOWLEDGMENTS

The authors thank Ari Jokinen, David Jenkins, and Kari Peräjärvi for their valuable comments. This work has been supported by the Academy of Finland under the Finnish Centre of Excellence Programme 2006-2011 (Project No. 213503, Nuclear and Accelerator Based Physics Programme at JYFL) and by the US Department of Energy under Grant No. DE-FG02-93ER40773. A.S. acknowledges the support from the Jenny and Antti Wihuri Foundation and the Magnus Ehrnrooth Foundation. J.C.H. is also supported by the Robert A. Welch Foundation under Grant No. A-1397. P.J.W. and T.D. would like to acknowledge support from the STFC.

[1] J. Jose *et al.*, Nucl. Phys. A **777**, 550 (2006).
[2] D. C. Black, Geochim. Cosmochim. Acta **36**, 347 (1972).
[3] A. F. Iyudin *et al.*, Astron. Astrophys. **300**, 422 (1995).
[4] R. Diehl *et al.*, New Astron. Rev. **52**, 440 (2008).
[5] A. F. Iyudin *et al.*, Astron. Astrophys. **443**, 477 (2005).
[6] S. Bishop *et al.*, Phys. Rev. Lett. **90**, 162501 (2003).
[7] B. Davids *et al.*, Phys. Rev. C **68**, 055805 (2003).
[8] A. Banu *et al.*, in *Proceedings of Nuclei in the Cosmos X*, PoS(NIC X) 052 (2008).
[9] A. Banu *et al.*, arXiv:1104.0675 [nucl-ex].
[10] T. Al Abdullah *et al.*, Phys. Rev. C **81**, 035802 (2010).
[11] S. Seuthe *et al.*, Nucl. Phys. A **514**, 471 (1990).
[12] S. Schmidt *et al.*, Nucl. Phys. A **591**, 227 (1995).
[13] R. J. Tighe, J. C. Batchelder, D. M. Moltz, T. J. Ognibene, M. W. Rowe, J. Cerny, and B. A. Brown, Phys. Rev. C **52**, R2298 (1995).
[14] F. Stegmüller *et al.*, Nucl. Phys. A **601**, 168 (1996).
[15] K. Peräjärvi *et al.*, Phys. Lett. B **492**, 1 (2000).
[16] D. G. Jenkins *et al.*, Phys. Rev. Lett. **92**, 031101 (2004).
[17] V. E. Iacob *et al.*, Phys. Rev. C **74**, 045810 (2006).
[18] A. Sallaska *et al.*, Phys. Rev. Lett. **105**, 152501 (2010).
[19] C. Rowland *et al.*, Astrophys. J. **615**, L37 (2004).

[20] L. Erikson *et al.*, Phys. Rev. C **81**, 045808 (2010).
[21] C. Iliadis *et al.*, Astrophys. J. Suppl. Ser. **142**, 105 (2002).
[22] S. Kubono *et al.*, Z. Phys. A **348**, 59 (1994).
[23] R. A. Gough *et al.*, Phys. Rev. Lett. **28**, 510 (1972).
[24] A. Ozawa *et al.*, Phys. Rev. C **74**, 021301(R) (2006).
[25] Y. Zhai, Ph.D. thesis, Texas A&M University, 2007.
[26] R. E. Tribble *et al.*, Nucl. Phys. A **701**, 278c (2002).
[27] R. G. Sextro, R. A. Gough, and J. Cerny, Phys. Rev. C **8**, 258 (1973).
[28] J. F. Ziegler [http://www.srim.org]
[29] R. Brun and F. Rademakers, Nucl. Instrum. Meth. Phys. Res. Sect. A **389**, 81 (1997).
[30] K. Peräjärvi (private communication).
[31] G. Audi, A. H. Wapstra, and C. Thibault, Nucl. Phys. A **729**, 337 (2003).
[32] M. Mukherjee *et al.*, Eur. Phys. J. A **35**, 31 (2008).
[33] A. Saastamoinen *et al.*, Phys. Rev. C **80**, 044330 (2009).
[34] R. B. Firestone, Nucl. Data Sheets **108**, 1 (2007).
[35] H. Nann, A. Saha, and B. H. Wildenthal, Phys. Rev. C **23**, 606 (1981).
[36] M. Bhattacharya *et al.*, Phys. Rev. C **77**, 065503 (2008).
[37] A. Sallaska *et al.*, Phys. Rev. C **83**, 034611(2011).
[38] B. Cederwall *et al.*, Nucl. Instrum. Meth. Phys. Res. Sect. A **354**, 591 (1995).
[39] V. E. Iacob *et al.*, Phys. Rev. C **74**, 015501 (2006).
[40] C. Angulo *et al.*, Nucl. Phys. A **656**, 3 (1999).
[41] R. D. Horansky *et al.*, J. Appl. Phys. **107**, 044512 (2010).